

## RESEARCH ARTICLE

# Locomotion- and mechanics-mediated tactile sensing: antenna reconfiguration simplifies control during high-speed navigation in cockroaches

Jean-Michel Mongeau<sup>1,\*</sup>, Alican Demir<sup>2</sup>, Jusuk Lee<sup>2</sup>, Noah J. Cowan<sup>2</sup> and Robert J. Full<sup>3</sup>

<sup>1</sup>Biophysics Graduate Group, University of California, Berkeley, CA 94720, USA, <sup>2</sup>Department of Mechanical Engineering, Johns Hopkins University, MD 21218, USA and <sup>3</sup>Department of Integrative Biology, University of California, Berkeley, CA 94720, USA

\*Author for correspondence (jmmongeau@berkeley.edu)

### SUMMARY

Animals can expend energy to acquire sensory information by emitting signals and/or moving sensory structures. We propose that the energy from locomotion itself could permit control of a sensor, whereby animals use the energy from movement to reconfigure a passive sensor. We investigated high-speed, antenna-mediated tactile navigation in the cockroach *Periplaneta americana*. We discovered that the passive antennal flagellum can assume two principal mechanical states, such that the tip is either projecting backward or forward. Using a combination of behavioral and robotic experiments, we demonstrate that a switch in the antenna's state is mediated via the passive interactions between the sensor and its environment, and this switch strongly influences wall-tracking control. When the tip of the antenna is projected backward, the animals maintain greater body-to-wall distance with fewer body collisions and less leg–wall contact than when the tip is projecting forward. We hypothesized that distally pointing mechanosensory hairs at the tip of the antenna mediate the switch in state by interlocking with asperities in the wall surface. To test this hypothesis, we performed laser ablation of chemo-mechanosensory hairs and added artificial hairs to a robotic antenna. In both the natural and artificial systems, the presence of hairs categorically increased an antenna's probability of switching state. Antennal hairs, once thought to only play a role in sensing, are sufficient for mechanically reconfiguring the state of the entire antenna when coupled with forward motion. We show that the synergy between antennal mechanics, locomotion and the environment simplifies tactile sensing.

Key words: biomechanics, running, *Periplaneta americana*, sensorimotor integration, bio-inspired sensor, robot.

Received 5 December 2012; Accepted 29 August 2013

### INTRODUCTION

Animals can directly control the acquisition of sensory information by using self-generated energy via muscle action to control their sensor, a process termed 'active sensing' (Bajcsy, 1988; Nelson and MacIver, 2006). Active sensing systems are characterized as information seeking (Prescott et al., 2011). From these definitions arise a common theme, the control of a sensor to suit the task. The energy for active sensing may come from muscles directly controlling the sensor, the body, or both. Research in active tactile sensing that has focused on slow, exploratory tasks such as sniffing in lobsters (Koehl et al., 2001), whisking in rats (Hartmann, 2001) and antenna-mediated exploration in invertebrates (Staudacher et al., 2005; Okada and Toh, 2004), has shown the importance of integrating knowledge of the sensor, body and environment to understand how animals can exert active control over their sensor to tune the gain, phase and spatial direction of the signal for acquiring information. Animals during slow, exploratory tasks rely predominantly on distributed neural feedback from sensors to execute effective control actions via the direct regulation of motor activity and subsequent actuation of the sensor and/or body (Chiel et al., 2009).

When animals are involved in extremely rapid control tasks such as predatory escape, where the neuromechanical system is pushed near its operating limit due to neural conduction delays (More et al., 2010), sensorimotor control bandwidth constraints impose fundamental limits on the gains that can be achieved for stable

closed-loop control (Cowan et al., 2006; Elzinga et al., 2012). In such cases, animals require a well-tuned control system to compensate for the delays and locomotor dynamics, thus relying on shared processing between the neural and mechanical system (Cowan et al., 2006; Holmes et al., 2006). Sharing processing loads further, biomechanical sensory structures themselves can mechanically process sensory information prior to neural transduction (Sane and McHenry, 2009). In some cases, these properties can simplify downstream neural computations by performing mechanical computations on the incoming stimulus before sensory transduction. For example, in echolocation in bats, the mechanics of the pinnae and tragi acts as a filter allowing bats to determine the elevation angle of prey (Wotton et al., 1995). In flies, the geometry and wiring of photoreceptors in the eye simplify optical flow computations (Egelhaaf et al., 2002). In barn owls, asymmetries in the arrangement of the facial ruff play a crucial role in sound localization (Coles and Guppy, 1988).

Here, we examined whether animals use the self-generated energy from locomotion to control the state of their sensor when their neuromechanical system is pushed near its limit during escape. Animals under these conditions could benefit from having tuned passive mechanical sensory structures adapted to their natural environment to simplify control by reconfiguring the sensor's state parameters according to the sensing strategy (Bajcsy, 1988) (Fig. 1A). We abstract this reconfiguration by showing distinct mechanical states  $x_1$  and  $x_2$  which are 'switched' by an interaction

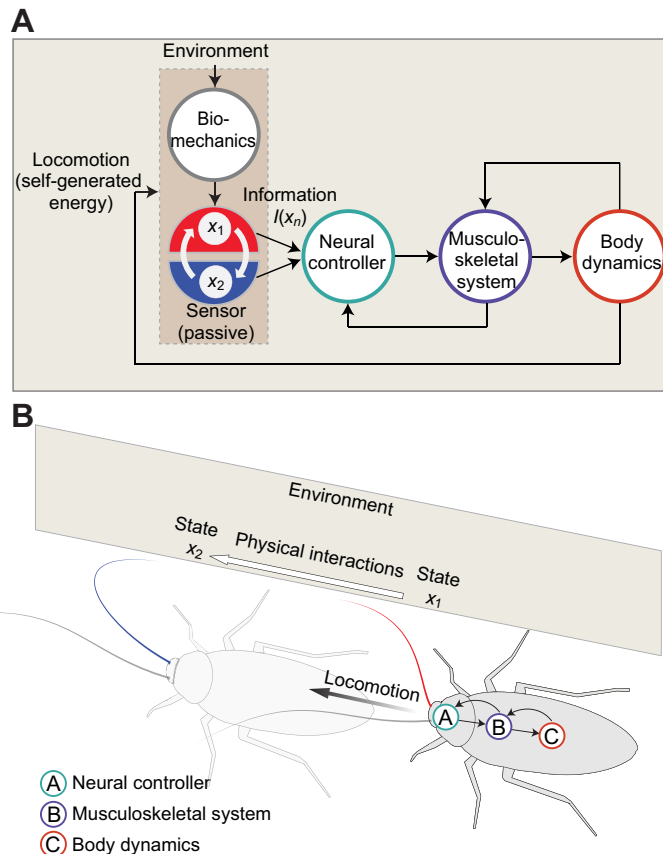


Fig. 1. Control diagram of locomotion-mediated tactile sensing with sensor reconfiguration *via* passive mechanics. (A) Abstraction of the interaction between an organism and its environment during the sensing task illustrated in B. The interaction between locomotion (the self-generated energy source), a passive sensor (darker shaded box) and the environment (lighter shaded box) processed through the biomechanics of a sensor can change the mechanical state of a sensor. The resulting distinct mechanical states of the sensor expressed by state parameters  $x_1$  and  $x_2$  can influence the information  $I(x_n)$  available to the neural controller. (B) Summary of evidence of locomotion-mediated tactile sensing for wall following in the American cockroach, *Periplaneta americana*. We illustrate that the physical interactions between a locomoting organism and its environment can lead to a reconfiguration (white arrow) of the sensor state [state  $x_1$  (forward) to state  $x_2$  (backward)] *via* passive mechanics. Arrows between the neural controller and musculoskeletal system indicate neural feedback whereas arrows between the body dynamics and musculoskeletal system indicate mechanical feedback.

between locomotion as the self-generated energy source, a mechanically tuned passive sensor and the environment. In turn, these states can affect the information  $I(x_n)$  available to the neural controller that generates movement.

To explore the interaction between locomotion, passive sensors and the environment, we studied thigmotaxis in cockroaches, *Periplaneta americana*, during blinded high-speed wall following where they employ their antennae. During wall following, cockroaches use their antennae to sense obstacles such as walls and control their body by executing rapid turns (Camhi and Johnson, 1999). While the natural habitat of *P. americana* is uncertain, these artificial walls represent extended obstacles that may be relevant to the natural ecological context of the genus *Periplaneta* in the form of caves and/or large rocks (Bell et al., 2007). Its hypothesized cave-like native environment is likely one reason this species predominantly adopts present-day, human-made structures such as dwellings (Seelinger, 1984). It has been hypothesized that to avoid collisions with extended obstacles such as walls, these animals can control or track their relative distance to the wall effectively, even at very high speeds (Cowan et al., 2006). For task-level control of this behavior, cockroaches use information predominantly from the flagellum, the long (up to 1.3 times body length), unactuated part of the antenna. Cockroaches can initiate a turn in response to a wall projection in less than 30 ms, leaving little time available for processing by the nervous system (Camhi and Johnson, 1999). This sensorimotor delay is within the range of rapid turns in other insects such as 90 deg turns in fruit flies (50 ms) (Dickinson, 2005) and turns in prey pursuit in dragonflies (33–50 ms) (Olberg et al., 2000). Moreover, it appears that cockroaches hold the angle of their antennae relative to their body midline relatively constant during high-speed wall following (Camhi and Johnson, 1999; Cowan et

al., 2006), and thus whole-body motions dominate sensory movements. This contrasts with low-speed exploration tasks in which local joint activity dominates sensory motion (Okada and Toh, 2000). Distributed along cockroach flagella is a vast array of mechanosensors that include hair sensillae and campaniform sensillae. The antennal nerve relays information from over 270,000 sensors, forming a vast network of exteroceptive and interoceptive sensors (Schafer and Sanchez, 1973; Schaller, 1978). It has been shown that a proportional-derivative (PD) controller operating on a whole-body or template model is sufficient to reliably predict wall-following behavior (Cowan et al., 2006). Furthermore, this controller is sufficient for task-level control when integrated into a more dynamically representative model of running (Lee et al., 2008).

Here, we demonstrate that during wall following in cockroaches, an antenna's mechanical state can be switched between two states based on wall roughness (Fig. 1B). First, we show evidence that the change in mechanical state of the antenna – which we characterize as projecting 'forward' or 'backward' – is mediated passively *via* interactions between the antenna and the environment. We compare the frequency of states for cases when the surface is smoother *versus* rougher, effectively pushing the mechanical performance of the antenna. Second, we show that this change in state affects control and performance. Specifically, the mechanical state of the antenna affects the body-to-wall distance – the proposed state variable for control – which in turn has implications for performance and control strategy. Therefore, a dynamic change in the state of the sensor results in changes in tracking. Third, we show that passive mechanical hair sensillae on the antenna are sufficient for mediating a change in the overall mechanical state of the antenna; that is, from its resting position to projecting 'backward'. This conclusion was reached through a set of experiments in which the hairs are ablated

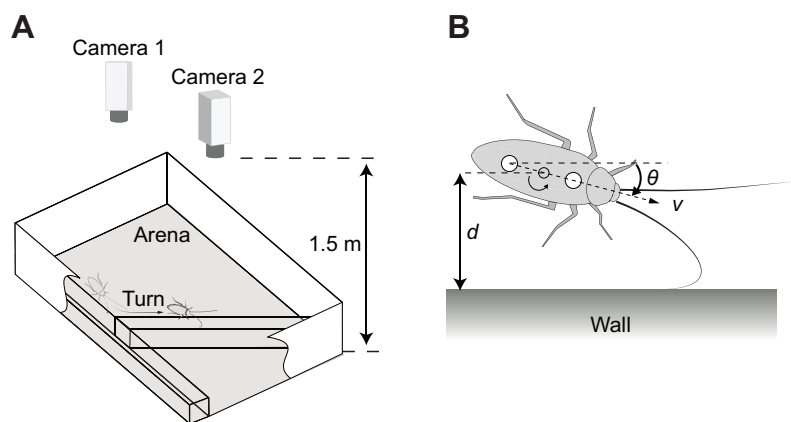


Fig. 2. Experimental setup to study high-speed wall following. (A) Arena with a turn perturbation for eliciting high-speed escape and wall following in *P. americana*. We recorded the time prior to and after a turn using two synchronized high-speed video cameras. Image adapted from Cowan et al. (Cowan et al., 2006). (B) Kinematic parameters evaluated for wall following. We digitized the two markers on the cockroach body (large white circles) to extract the point of rotation (POR; small circle with arrow) and body angle  $\theta$  relative to the wall.  $v$  is the forward velocity of the animal;  $d$  is the distance between the body and the wall.

with a high-precision laser system and was corroborated independently by testing the role of artificial antennal hairs added to a tunable physical model inspired by arthropod antennae. We show that large mechanosensory hairs play a crucial mechanical role in mediating sensor reconfiguration; thus, we propose a novel function for these structures, previously described as having an exclusively sensory function.

## MATERIALS AND METHODS

### Animal husbandry

Adult male American cockroaches, *Periplaneta americana* (Linnaeus 1758), were acquired from a commercial vendor (Carolina Biological Supply Company, Burlington, NC, USA) and housed in plastic cages maintained at a temperature of 27°C. Cockroaches were exposed to a 12 h:12 h light:dark cycle and given fruits, dog chow and water *ad libitum*.

### Arena for turn perturbation

We built a rectangular arena as described elsewhere (Cowan et al., 2006) (Fig. 2A). Within the rectangular arena (85×45×15 cm length×width×height) we placed acrylic (smoother) and wood (rougher) blocks cut at angles of 30, 45 and 60 deg to induce turning in wall-following cockroaches. To capture the high-speed escape behavior, two high-speed video cameras (Kodak Ekta Pro 1000, Eastman Kodak Company, Rochester, NY, USA) were positioned 1.5 m above the area. Adjacent camera views overlapped to enable calibration and provide continuity of data for each trial sequence. Video sequences were synchronously captured at 500 frames s<sup>-1</sup> with an average resolution of 0.8 mm per pixel. To enhance contrast and tracking of cockroach body and legs, we used retroreflective sheets (3M, St Pauls, MN, USA) as the running substrate and placed retroreflective markers on the cockroach body.

### Animal preparation

Prior to running animals, we prepared each cockroach using a previously described protocol (Cowan et al., 2006). While cockroaches were anesthetized we taped two small round retroreflective dots dorsally aligned with the body fore–aft axis. The dots were placed directly over the wings but did not restrict their motion. These two dots allowed us to estimate the cockroach position and heading vector from the high-speed videos. To prevent visual cues from influencing wall-following behavior, we covered the compound eyes and ocelli with white nail polish while carefully avoiding the head/scape joint. Following the preparation we allowed cockroaches at least 24 h for recovery at room temperature prior to conducting experiments.

### Kinematics

We used the camera calibration procedure described previously (Cowan et al., 2006) for digitization. For each frame, we digitized the two markers on the cockroach body to extract the point of rotation (POR) and body angle (Fig. 2B). The procedure for determining the POR is described elsewhere (Cowan et al., 2006) and involves performing a least-square fit using the velocity and angular velocity for two consecutive frames assuming cockroaches run like an ideal no-slip planar unicycle. Here, we used the POR metric solely as a body reference to estimate body-to-wall distances of cockroaches. We filtered the position data using a zero-phase low-pass Butterworth filter with a cut-off frequency of 62.5 Hz, which corresponds to a frequency nearly three times the fastest turning rates described in cockroach wall following (Camhi and Johnson, 1999). We accepted all trials when the animals rapidly followed the wall and executed a turning response when contacting the angled wall, but excluded trials when animals tried to climb the wall or stopped. Trials were rejected when the distance of the POR to the wall exceeded 2.5 cm while the cockroaches were running along the angled wall.

### Wall properties

To determine the relationship between wall roughness and antenna configuration, we manually tracked videos of running cockroaches encountering a turn perturbation with smoother acrylic walls and rougher wood walls. We recorded the initiation of a stride by manually determining the onset of stance initiation of the hindleg contralateral to the wall perturbation. We rejected strides when the antenna position could not be clearly determined to be either projecting forward or backward for the entire stride (4% of strides). We also rejected strides when the antenna was not in contact with the wall for at least 80% of the stride (35% of strides) to ensure sufficient interaction between the antenna and the wall. In these rejected strides, the animals would often steer away from the wall, which would then cause the ipsilateral antenna to momentarily lose contact with the wall. We defined an antenna ‘flip’ as when an antenna moved from a forward-projecting to a backward-projecting position and *vice versa*. Only animals ( $N=8$  animals total) with at least 15 accepted strides were included in the final analysis. Besides wall roughness, another parameter that could possibly affect the distribution of antenna states is the antennal joint angles. While previous studies suggest little variation in antenna angles and little-to-no contribution from basal segments during wall following (Camhi and Johnson, 1999), we measured whether animals could actively modulate antennal joint angles as a control. We randomly sampled trials within our dataset for smoother and rougher walls.

We sampled 98 strides following the turn perturbation ( $N=6$  animals in total: 3 on rough, 3 on smooth; 12 trials total: 6 on rough walls, 6 on smooth) and found no statistically significant changes in per-stride body–antenna (ipsilateral) angle ( $t$ -test,  $P=0.99$ ) and inter-antennal angle ( $t$ -test,  $P=0.74$ ) between smoother and rougher walls. These changes remained insignificant even after correcting for the possible effect of individual animals (mixed-effect model,  $F$ -test, body–antenna angle  $P=0.95$ , inter-antenna angle  $P=0.67$ ). Therefore, we did not include this parameter in explaining the variation in antenna state.

#### Wall contact

To determine the effect of the antenna state on body-to-wall distance, we ran a separate set of animals using the same track. We selected trials before the turn perturbation with clearly identifiable antenna positions (either projecting forward or backward) and computed the shortest distance between the POR and a vector from points on the wall using custom-written scripts (Matlab, The MathWorks Inc., Natick, MA, USA). We categorized the effect of body-to-wall distance on wall-following performance by manually tracking the videos of running cockroaches on a stride-to-stride basis. We determined the initiation of a stride by manually determining the onset of stance initiation of the hindleg contralateral to the wall perturbation. We rejected strides when (1) the antenna position could not be clearly determined to be either projecting forward or backward projecting for the entire stride (8% of all strides), (2) the antenna was not in contact with the wall for at least 80% of the stride (29% of all strides), and (3) the antenna flipped (either forward or backward; 17% of all strides). For each stride, we manually recorded evidence of leg contact by the tibia and femur joints (excluding contact of the tarsal segment) as well as evidence of body (head, thorax and/or abdomen) contact with the wall.

#### Tracking control

We quantified the effects of backward-to-forward antenna flips on wall-following control by manually identifying flips within our dataset after cockroaches encountered the turn perturbation. We recorded the frame at the onset of the flip for each instance. We rejected all events when the antenna flip was initiated by the cockroach turning; that is, when the body angle was greater than or equal to  $\pm 15^\circ$  from the wall within the stride when the flip occurred. This occurred in 5% of flips (1/19). We estimated the stride time ( $\sim 80$  ms) by taking the reciprocal of the median stride frequency ( $11.9 \text{ strides s}^{-1}$ ). For each flip, we normalized the body angle of the animals by their respective averages  $\sim 1$  stride prior to the flip (80 ms). Body angles were computed by taking the arctangent between the vector formed by the two dots on the animal's body and the reference wall vector (Fig. 2B). We then analyzed the normalized body angles  $\sim 3$  strides (240 ms, one stride  $\sim 80$  ms) after the onset of the flip. To determine any significant effect of these flip events on wall-following control, we compared these kinematic variables with control sequences with no antenna flips by randomly selecting trials 240 ms after turning (average timing of flip occurrences after turn) within a 100 ms window downstream of the turn. The same body angle normalization procedure was applied to the control dataset. To determine statistical significance between the two groups, we applied a statistical mixed-effect model of the form  $\text{abs}(\text{angle}) = \text{time} + \text{animal} + \text{group} + (\text{animal} \times \text{time}) + (\text{group} \times \text{time})$  where  $\text{abs}$  is the absolute value, angle is the angle measurement at each time point (2 ms interval), animal is a random factor and group is a fixed effect (flip *versus* control). To determine whether the statistical result was sensitive to the possible effect of a small sample

size and a non-normal distribution, we calculated 95% confidence intervals on bootstrapped means for both groups using 1000 replications. We compared the bootstrapped means from an original sample of 18 flip events and 30 control events.

#### Passive antenna reconfiguration – biological experiments

We measured the effect of passive hairs on the antenna state by developing a technique using a diode-pumped Q-switched micromachining laser (Matrix 355, Coherent, Santa Clara, CA, USA) to ablate hair arrays on each antennal annuli. High-precision laser ablation has been successfully used on arthropods in the past; for example, to ablate genital hairs in *Drosophila bipectinata* (Polak and Rashed, 2010). Hairs on individual annuli were ablated by pulsing the laser at a frequency of 20 kHz while drawing a rectangle the size of each annulus at  $10 \mu\text{m}$  spacing at a speed of  $250 \text{ mm s}^{-1}$ . For each annulus, coordinates were manually defined at  $1 \mu\text{m}$  resolution to avoid hitting the intersegmental membranes. We ablated hairs of the first 10 distal annuli in head- and antenna-fixed animals in both the dorsal and ventral directions. We found that orienting the antenna with dorsal and ventral side up was sufficient to ablate hairs circumferentially. We acquired high-magnification ( $25\text{--}50\times$ ) images of individual annuli under a microscope in both the dorsal and ventral direction to determine the quality of the ablation process. After ablation, under a high-magnification microscope, we observed that the treated portion of the antenna retained hemolymph flow and that the cockroach responded to touch on the treated antenna. To demonstrate the effect of antenna hairs, we compared the performance of ablated and non-ablated antenna when sliding along a surface (Fig. 3A). After cold-anesthetizing the animals by placing them in glass beakers on ice for 30 min (thus avoiding direct contact with the ice), we used staple pins to mount the animal on a gel plate and fixed the head and base of the antenna with dental silicone (President light body, Coltène, Altstätten, Switzerland). We fixed the base of the antenna at an angle of  $30^\circ$  relative to the body long axis, which is similar to the angle observed in wall following (Camhi and Johnson, 1999). The candidate antenna was allowed to rest freely against a paraffin plate. The paraffin plate was made by melting paraffin on a glass plate placed on a hot plate. Because of surface tension, the paraffin melted and created a thin coat of wax. The plate was attached to a linear micro-translation stage (M112.1DG, Physik Instrumente, Palmbach, Germany). After carefully allowing the antenna to come into contact with the wall under a microscope with the antenna in a forward-projecting position, we drove the wall towards, but parallel to, the cockroach at a speed of  $2 \text{ mm s}^{-1}$  over a distance of 2.5 cm (Fig. 3B). To control for the possible effect of antenna contact area biasing our results, we varied the initial conditions such that the antenna was initially mounted with 1–10 annuli in contact with the wall. To control for surface irregularities on the wall, we randomized the initial position of the antenna against the wall for all annulus numbers. We observed and noted whether the antenna flipped and measured the frequency for each condition from high-resolution video recordings of each trial under a microscope. After a trial, we measured the antenna length from the scape to the last annulus of the flagellum. To test whether the angle of attack of the flagellum could affect the likelihood of reconfiguration or flipping, we repeated this experiment with abduction angles of  $15^\circ$ ,  $50^\circ$  and  $70^\circ$  with non-treated, control antennae.

#### Passive antenna reconfiguration – physical model of antenna

We tested the sufficiency of passive hairs in changing the antenna state by adding artificial hairs to a highly tunable and modular



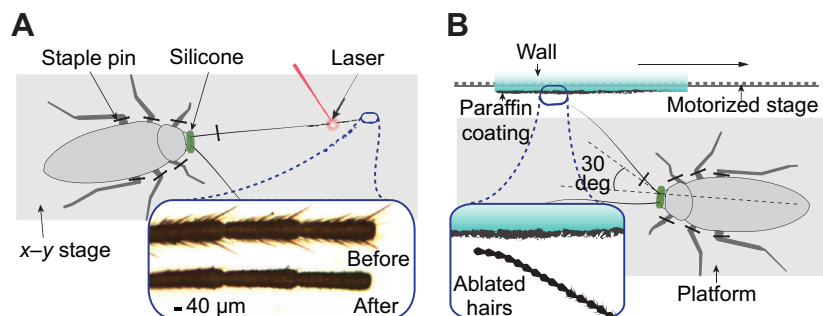


Fig. 3. Methods for determining the mechanical role of hairs. (A) Procedure for laser hair ablation. The body and antennae of cockroaches were restrained on an x-y stage while we applied laser pulses at the tip of the antenna on both the ventral and dorsal sides. The inset shows high-resolution images of the three distal-most annuli of a cockroach antenna viewed from the ventral position. The top image shows the antenna before hair ablation and the bottom image shows the same antenna annuli after laser hair ablation. (B) Experimental procedure for determining the role of hairs in reconfiguring the antenna. We mounted body- and antenna-fixed animals on a platform and allowed the tip of the antenna to slide along a rough (paraffin) wall mounted on a motorized stage. The inset shows a drawing of a treated antenna prior to interacting with the wall.

physical model inspired by arthropod antennae (Demir et al., 2010). To approximate the stiffness distribution of insect antennae (Staudacher et al., 2005), we designed an eight-segment model with tunable joint stiffness. We ran our eight-segment ( $8 \times 40$  mm) robotic antenna with a constant base velocity  $v_{\text{base}}$  of  $15 \text{ mm s}^{-1}$  against a wall (Fig. 4A). In the middle of each segment, we placed an 18 mm long anisotropic ‘hair’ protruding at  $45^\circ$  towards the distal end of the antenna (Fig. 4B). The hairs were anisotropic, which is a known biomechanical feature of the thick-wall chemosensory/mechanosensory sensilla (chaetica B) of the cockroach *P. americana* (Schafer and Sanchez, 1973). Here, anisotropy refers to the direction in which a hair can collapse.

We performed a total of seven experiments each with 10 trials (total of 70 trials). For each trial the base angle  $\theta$  was set to  $30^\circ$  and the distance to the wall,  $d$ , from the antenna base was kept at 135 mm. As an initial condition, the robotic antenna posture was always projecting in the direction of motion (forward). The forward velocity of the base was determined such that the antenna was at a quasi-static state in motion to minimize inertial effects. The linear actuator was a belt-driven Velmex BiSlide (Velmex Inc., Bloomfield, NY, USA) with a resolution of  $25 \mu\text{m}$  and a travel distance of 1 m. Antenna segment data were sampled via a common I2C bus facilitated by a 600 MHz Gumstix Verdex Pro (Gumstix Inc., Portola Valley, CA, USA) base computer. Both the linear actuator and the base computer were controlled asynchronously by custom-designed client software. We recorded each segment joint angle with a resolution of  $0.35^\circ$  at a rate of 120 Hz.

Fig. 4C is a computer-aided design (CAD) rendering of the antenna segment showing the hair design. Two hairs (Fig. 4C, 2) – one at each side – can be placed per segment on one of the two available cylindrical extrusions, about which the hair is free to rotate (Fig. 4C, 5). We designed two different hair types, where one is projecting distally and the other proximally. These two types mirror each other about the segment’s sagittal plane and thus determine in which direction they are free to collapse. A distally (or likewise, a proximally) projecting hair can be at most  $45^\circ$  from the segment after which a mechanical hard stop is encountered (Fig. 4C, 3). Each hair is also spring-loaded to swing open (to  $45^\circ$ ) by a  $0.1 \text{ mm}$  diameter nickel–titanium (nitinol) wire, which simultaneously acts as the pointy hair tip that ‘anchors’ into the wall surface (Fig. 4C, 1). The hair was placed such that in the event of a collapse, it would trigger the contact sensor (Fig. 4C, 6).

During a trial, when a distally oriented hair was anchored to asperities in the wall, the entire antenna went into a transition phase which can result in a flip, where the antenna switches to a backwards-projecting configuration. We define a flip as a successful transition in which the most distal segment angle exceeds  $90^\circ$  with respect to the wall.

A base angle of  $30^\circ$  was chosen to be consistent with prior studies of rapid wall following in *P. americana* (Camhi and Johnson, 1999; Cowan et al., 2006). Additional control trials were conducted at  $10^\circ$ ,  $20^\circ$ ,  $60^\circ$  and  $70^\circ$  to test the sensitivity of flipping to the base angle. For each angle, we maximized the distance to the wall while ensuring that the final antennal segment contacted the wall. During each trial, we recorded whether the hairs disengaged from the wall before the antenna flip occurred.

### Statistical analysis

We performed all statistical analysis of our data using the statistics toolbox in Matlab (The MathWorks Inc.) and Minitab (Minitab Inc., State College, PA, USA). Bootstrapping was applied by randomly resampling with replacement.

## RESULTS

### Wall properties change state of antenna

To determine the interactions between the ipsilateral antenna and the environment (wall surface) during high-speed wall following, we ran male cockroaches along both smoother (acrylic) and rougher (wood) wall surfaces in an arena with a turn perturbation (Fig. 2A). We accepted a total of 259 strides from 39 trials with  $N=3$  animals running along smoother walls (body length  $3.57 \pm 0.2 \text{ cm}$ , ipsilateral antenna length  $4.10 \pm 0.4 \text{ cm}$ , mean  $\pm$  s.d. unless otherwise noted). We accepted a total of 354 strides from 40 trials with  $N=5$  animals running along rougher walls (body length  $3.60 \pm 0.2 \text{ cm}$ , ipsilateral antenna length  $4.42 \pm 0.4 \text{ cm}$ ). The combined group of animals ran with a mean speed of  $37.8 \text{ cm s}^{-1}$ , ranging from  $34.8$  to  $41.1 \text{ cm s}^{-1}$ . Speed was not significantly different between the two groups ( $t$ -test,  $P=0.15$ ). During these experiments, we observed antennae using a 2D dorsal projection to determine the antenna tip’s flipped state between being forward and backward projecting and *vice versa* as the antenna interacted with the wall (Fig. 5A). We found these ‘backward’ and ‘forward’ states to be the dominant antenna configurations, persisting for many strides. In the backward-projecting configuration, most of the flagellum was typically out in front of the animal, but the tip was projecting rearward, so the

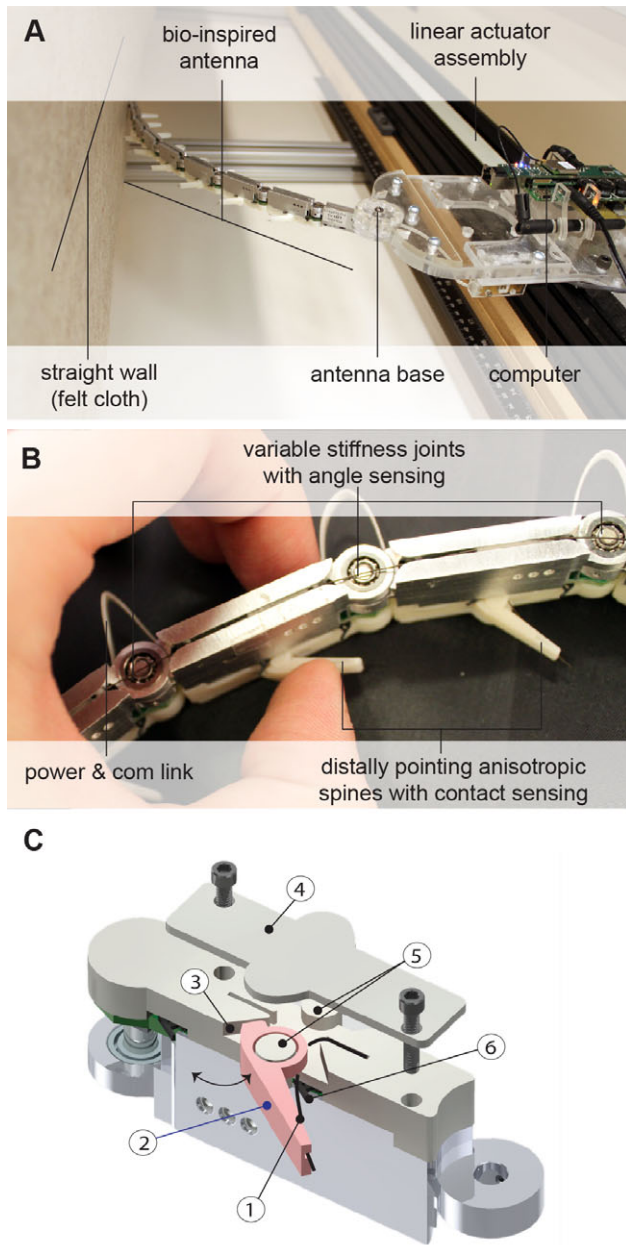


Fig. 4. Physical model of the antenna. (A) Physical model for independently testing the hypothesis that hairs facilitate the passive reconfiguration of an antenna. The eight-segment robotic antenna with anisotropic hairs is tangent to a felt-cloth-covered wall in the forward-projecting posture. (B) Close-up of the robotic antenna showing the inter-segmental joints and the collapsing direction of a hair. (C) Computer-aided design (CAD) rendering of a single antenna segment with anisotropic hairs: (1) NiTi hair tip and stiffness element; (2) hair; (3) hair 45 deg hard stop; (4) segment cover; (5) hair slots; (6) contact sensor.

flagellum assumed an inverted-J shape. When comparing wall-following performance for the two groups, we found that animals encountering rougher walls had their antennae projecting backward more often than animals running along smoother acrylic walls (smoother 51%, rougher 85%; Fig. 5B). Similarly, for animals following smoother walls, the ipsilateral antennae assumed a forward position more often than animals running along rougher walls (smoother 26%, rougher 1%). Antennae ‘flipped’ (either forward to backward or backward to forward) at similar frequencies

for the two wall surfaces (smoother 11%, rougher 14%). When comparing the proportion of forward *versus* backward antennal positions during a stride (excluding strides when the antenna flipped), we found that four out of five individuals never had a forward-projecting antenna on the rougher surface (0/34, 0/48, 0/17, 0/102), and only one individual showed five instances in 102 strides. By contrast, all individuals following smoother walls showed a large proportion of strides with forward-projecting antennae (16/83, 40/95, 15/23). We found a significant association between wall properties and the state of the antenna (Pearson  $\chi^2$ -test,  $P < 0.001$ ). To investigate antenna flips further, we calculated transition probabilities within and between states by treating antenna positions as a two-state discrete Markov chain (Fig. 5C). We found that if the antenna was in a forward state on smoother walls, the probability that it remained in that state in the next stride was 93%, whereas if it was forward on rougher walls, it never remained in the forward state in the next stride. Given these observations suggesting that wall properties categorically influence antenna configuration, we investigated whether the antenna’s state affected task-level control.

#### Body-to-wall distance depends on state of antenna

To test the effect of the antenna’s mechanical state on wall-following control, we ran a separate set of male cockroaches ( $N=12$  animals; body length  $3.29 \pm 0.18$  cm; ipsilateral antenna length  $3.96 \pm 0.37$  cm) on both smoother and rougher wall surfaces. Animals ran with a mean speed of  $46.2 \text{ cm s}^{-1}$  that ranged from  $37.7$  to  $53.1 \text{ cm s}^{-1}$ . We analyzed 80 trials after a turn perturbation and divided the data into two groups based on the position or state of the antenna, and measured the body-to-wall distance for both groups (Fig. 2B), the putative control variable for wall following (Cowan et al., 2006). We found that animals with an antenna projecting forward following a turn perturbation ran significantly closer to the wall ( $12.0 \pm 1.72$  mm,  $N=18$  trials;  $t$ -test  $P < 0.001$ ) than those running with an antenna projecting backward ( $19.9 \pm 4.86$  mm,  $N=62$  trials) after including the effect of individuals (random factor) and running speed (covariate) using a mixed-effect model ( $F$ -test,  $P < 0.001$ ; Fig. 6A,B). This change in body-to-wall distance corresponds to approximately the body width of *P. americana*. We found that the variance between the two groups was significantly different ( $F$ -test for equivariance,  $P=0.002$ ). As running speed has been shown to be correlated with body-to-wall distance (Camhi and Johnson, 1999), we tested for the effect of speed. We found no significant difference in running speed (backward  $44.8 \pm 8.22 \text{ cm s}^{-1}$ , forward  $41.0 \pm 7.35 \text{ cm s}^{-1}$ ) between the two groups ( $t$ -test,  $P=0.728$ ) even after correcting for the possible effect of individuals ( $F$ -test,  $P=0.792$ ).

#### Tracking performance depends on state of antenna

To determine possible effects of body-to-wall distance on running performance, we tracked individual strides of wall-following cockroaches running alongside rougher and smoother walls using the same dataset to measure body-to-wall distances presented earlier. We accepted a total of 129 strides with the ipsilateral antenna projecting forward and 231 strides with the antenna projecting backward. When comparing wall-following performance for cockroaches before and after a turn perturbation, we found that animals running with an antenna projecting forward had a significant increase in frequency of leg (tibia and/or femur) and body contact with the adjacent wall (Fig. 6C). The state of the antenna had a statistically significant association with leg contacts and body contacts (Pearson  $\chi^2$ -test,  $P < 0.001$  for both leg and body contacts). This association remained significant even after correcting for the possible effect of individuals (Cochran–Mantel–Haenszel test,

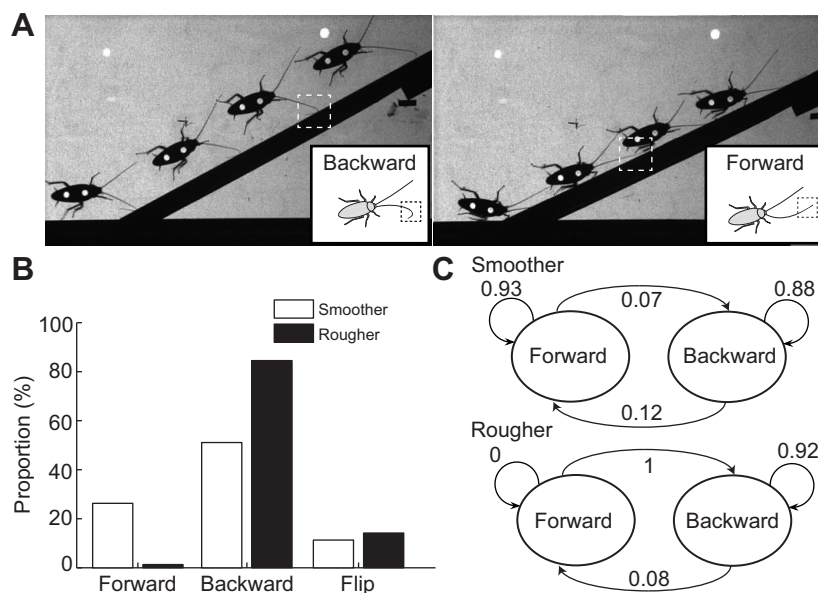


Fig. 5. Effect of wall properties on antenna mechanical state. (A) Two wall-following sequences during a turn perturbation recorded from high-speed video. The left panel shows a cockroach running with its antenna bent, projecting backward, whereas the right panel shows the same animal in a different trial running with the antenna straight, projecting forward. Wall properties are the same for the two trials. Boxes with dashed lines highlight the shape of the antenna as it interacts with the wall. (B) Proportion of antennae pointing forward, backward or flipping for smoother and rougher wall surfaces. Wall surfaces categorically affected the antenna state ( $P<0.001$ ). (C) Transition probabilities within and between states by modeling antenna reconfiguration as a two-state discrete Markov chain. Transition probabilities calculated from the transition matrices for both smoother and rougher walls are shown by arrows.

$P<0.001$  for both leg and body contacts). For strides where the body contacted the wall (35 strides total), these collisions often led to a decrease in speed, likely due to the impact. We found the median change in velocity to be  $-7.48\pm 6.84\text{ cm s}^{-1}$  when comparing approximately two strides before and after contact. We estimated the stride time (70.0 ms) by taking the reciprocal of the median stride frequency for all trials ( $14.3\text{ strides s}^{-1}$ ). Thus, animals slowed down after body contact on average. This change in speed following body contact is consistent with previous observations (Baba et al., 2010).

#### Change in antenna state affects tracking control

From behavioral observations, we hypothesized that a dynamic switch in state of the antenna affects control as evidenced by a change in body angle. We quantified one state change: a flip when the antenna moved from a backward to a forward position. To test the effect of antenna flips on wall-following control, we ran male cockroaches on rougher (wood) surfaces ( $N=11$  male cockroaches, body length  $3.70\pm 0.17\text{ cm}$ , mass  $0.77\pm 0.11\text{ g}$ , ipsilateral antenna length  $4.36\pm 0.41\text{ cm}$ ). Animals ran at a mean speed of  $46.2\pm 8.4\text{ cm s}^{-1}$ , which ranged from  $34.8$  to  $62.5\text{ cm s}^{-1}$ . We averaged body angles (Fig. 2B) for approximately three strides following a flip or no-flip control (Fig. 6D). We estimated the stride time (80.0 ms) by taking the reciprocal of the median stride frequency ( $11.9\text{ strides s}^{-1}$ ). Here, our control was defined as any randomly chosen time point in our wall-following dataset after a turn perturbation that was not flagged as a flip (see Materials and methods). Body angles greater than or equal to  $15^\circ$  suggest that a cockroach initiated a body turn (Camhi and Johnson, 1999). We found that flips occurred infrequently (18 strides with flips out of 676 strides). Using the mixed-effect model described in Materials and methods, we found that flips had a significant effect on body angle. Specifically, we found that the term group (intercept) and group $\times$ time (slope) were both statistically significant in our model ( $F$ -test,  $P<0.001$ ). This result remained significant after testing for a possible non-normal distribution of angles using a logarithmic transformation ( $F$ -test,  $P<0.001$ ). When comparing bootstrapped 95% confidence intervals of the normalized mean angles (absolute value) for both groups, we found no overlap [flip= $6.91$ – $9.69^\circ$ ; control= $4.91$ – $6.67^\circ$ ; Fig. 6E]. Applying the same test on angles without taking the absolute value did not change the statistical outcome.

#### Passive antenna reconfiguration – role of antenna hairs

We hypothesized that large chemo-mechanosensory hairs could allow the antenna to effectively stick to walls and mediate the transition from forward to backward bending. To determine the role of antenna hairs in mediating changes in antenna state, we developed a technique that allowed us to perform annulus-by-annulus hair ablation treatment on the first 10 annuli from the tip using a high-resolution micromachining laser (Fig. 3A). The results from one treatment are shown in Fig. 3A. We compared the performance of control ( $N=5$  animals, 50 trials; mass  $0.81\pm 0.09\text{ g}$ , antenna length  $4.24\pm 0.43\text{ cm}$ ) and experimental antennae ( $N=5$  animals, 50 trials; mass  $0.91\pm 0.06\text{ g}$ , antenna length  $4.35\pm 0.33\text{ cm}$ ) while sliding along a paraffin surface for head-fixed animals (Fig. 3B, Fig. 7A). During a flip, the hairs at the tip first engaged with the wall, causing the tip to stick. As the wall's motion progressed, the tip began to turn backward by twisting (Fig. 7A). With ablated hairs, the flagellum would catch but fail to engage and subsequently slip back into a forward-projecting state. We found a significant difference in flipping frequency between control and treated antennae (Pearson  $\chi^2$ -test,  $P<0.001$ ) (Fig. 7B). We found no effect of the number of annuli in contact with the wall on flipping frequency (Cochran–Mantel–Haenszel test,  $P<0.001$ ). Interestingly, contact of a single annulus with the wall often was sufficient for interlocking and subsequent flipping. For non-treated, control antennae ( $N=3$  animals with eight trials per angle; mass  $0.74\pm 0.04\text{ g}$ , antennal length  $4.8\pm 0.2\text{ cm}$ ), we found no significant effect of antennal abduction angle on the likelihood of flipping (Pearson  $\chi^2$ -test,  $P=0.36$ ) even after considering the possible effect of individuals (Cochran–Mantel–Haenszel test,  $P=0.37$ ).

#### Physical model tests biological hypotheses

To independently test the hypothesis that antenna hairs can mediate a change in state of the antenna when coupled with locomotion, we translated an eight-segment robotic antenna with a constant base velocity  $v_{\text{base}}$  of  $15\text{ mm s}^{-1}$  against the wall (Fig. 4A). Across the six experiments, we varied the wall surface and the hair orientation using the following combinations: (1) rough (felt-cloth) wall, distally pointing hairs; (2) rough wall, three distal segments with no hairs; (3) rough wall, proximally pointing hairs; (4) smoother (glossy paper) wall, distally pointing hairs; (5) smoother wall, three



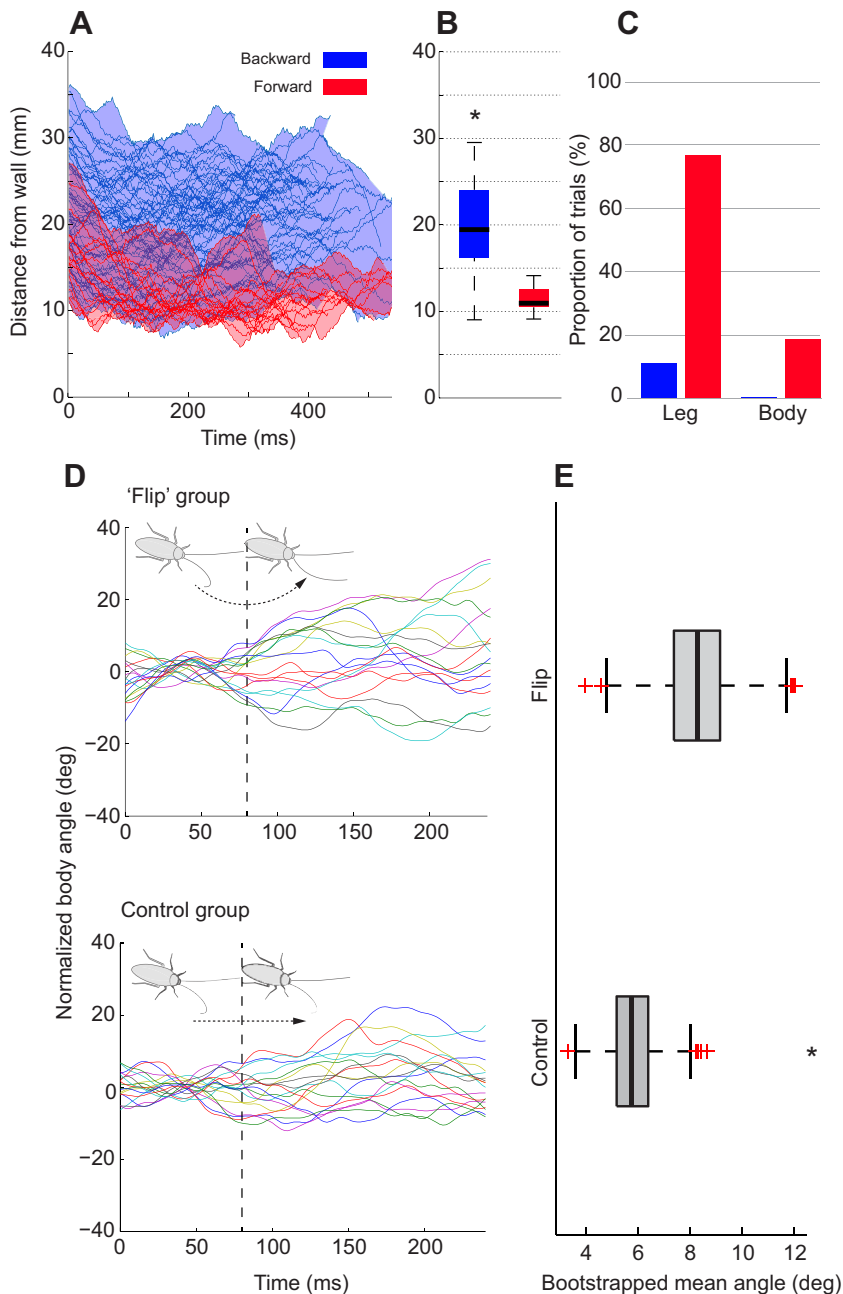


Fig. 6. Locomotor performance as a function of antenna mechanical state. (A) Body-to-wall distance of cockroaches wall following for antennae projecting backward or forward as a function of time following a turn perturbation. The shaded blue and red regions show the full range of body-to-wall distances while individual lines represent single trials. Animals running with an antenna projecting forward following a turn ran significantly closer to the wall than animals running with an antenna projecting backward. (B) The box plot summarizes body-to-wall distances shown in A for backward and forward groups ( $*P < 0.001$ ). (C) Proportion of trials where the leg and/or body contacted the wall for strides with forward- and backward-projecting antennae. Overall, the antenna state had a statistically significant association with the frequency of leg and body contacts ( $P < 0.001$ ). (D, top) Body angles for animals running while the antenna flipped from forward to backward projecting. Individual lines represent single trials. The vertical dashed line represents the onset of the antenna flip. (Bottom) Body angles for the non-flip control group. Individual lines are randomly selected trials where the antenna remained backward. The vertical dashed line represents randomly selected time events. Positive angles indicate the cockroach was turning away from the wall and negative angles indicate the cockroach was turning toward the wall. (E) The box plot summarizes the bootstrapped body angles (absolute value) following a flip and for non-flip controls. Angles were statistically significant when comparing 95% confidence intervals ( $*P < 0.05$ ). For box plots in B and E the central line is the median, the bottom and top edges of the box are the 25th and 75th percentiles and the whiskers extend to  $\pm 2.7$  s.d. Red crosses represent outliers lying outside whiskers.

distal segments with no hairs; (6) smoother wall, proximally pointing hairs. Proximally pointing hairs pointed towards the base whereas distally pointing hairs pointed away from the base.

In experiment 1, we observed that the hair tips of the distal segments anchored to the asperities of the rough (felt) material almost immediately. Fig. 7C illustrates data from one trial of experiment 1 where the antenna initiated a flip immediately after the smoother zone (glossy paper) of the wall. A similar response was observed for the remaining nine trials. For experiment 2, we removed the three distal hairs analogous to the laser ablation experiments for the real cockroach flagellum. We did not observe a flip in any of the 10 trials. In four out of the 10 trials, we observed 'catching' at the most distal segment, but these hair-substrate interactions were not enough to successfully flip the antenna. Fig. 7D shows data from one trial of experiment 2 where such a failed transition occurred. For experiment 3, we reversed the orientation of the hairs to evaluate the effects of the hair orientation. This control

would have been infeasible to test on a cockroach flagellum. In all 10 trials, the antenna did not flip. For all the other experiments (4–6) with the smoother wall, the antenna slid over the corresponding surface without initiating a flip. In some cases, the cockroach antenna changed state *via* torsion around the flagellum (Fig. 7A), but the robotic antenna could not flip *via* this mechanism (Fig. 7C,D); this degree of freedom was not available by design.

To complement experiment 1 (rough wall, distally pointing hairs), we conducted a control to determine whether flipping was sensitive to the base angle by repeating the experiment with base angles of 10, 20, 60 and 70 deg. In all trials, the antenna flipped from forward to backward. Specifically, the hairs never disengaged from the wall before flipping occurred. This suggests that antennal reconfiguration (flipping) is insensitive to base angle.

When a flip was completed with distally pointing hairs, the hairs pointed proximally and thus could not interlock with the asperities while forward motion progressed. We observed that the wall contact



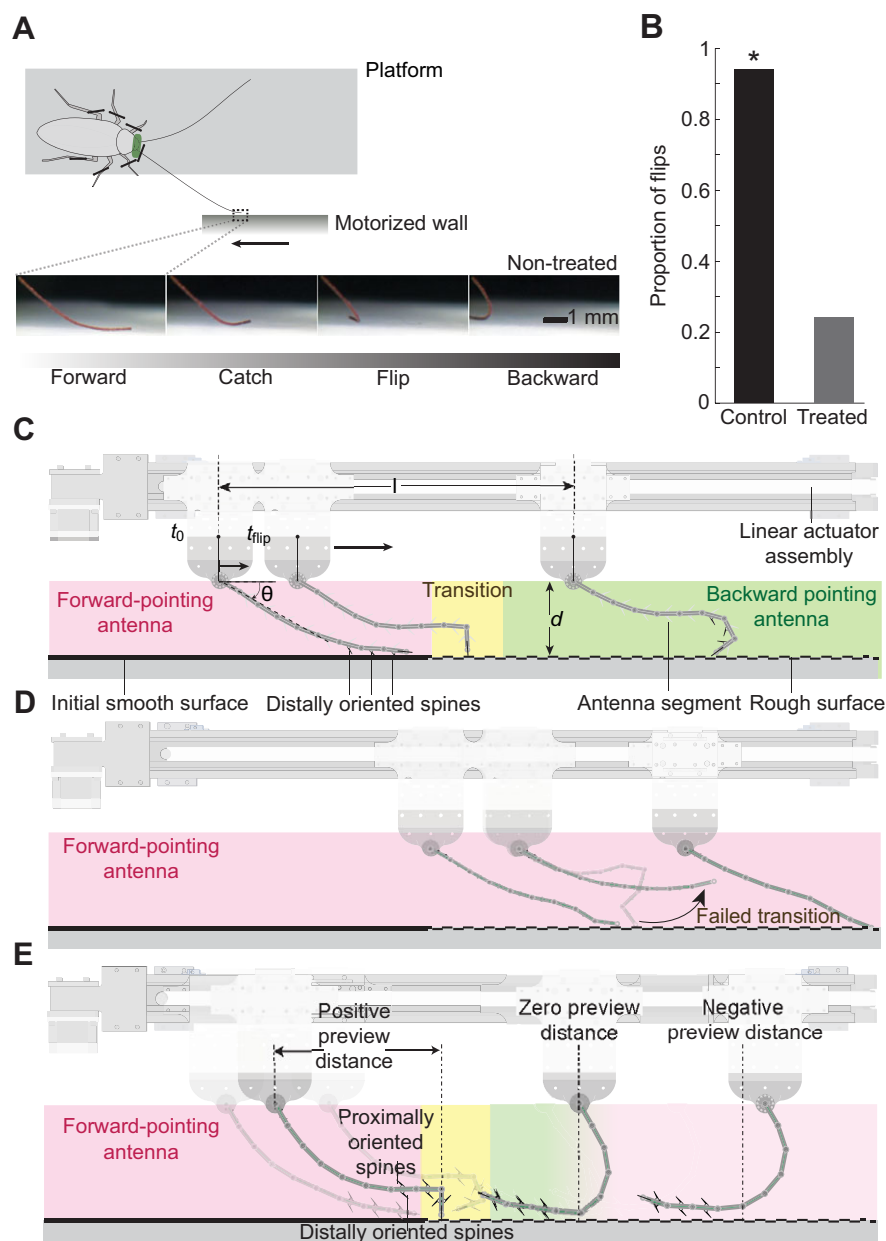


Fig. 7. Sufficiency of antenna hairs in mediating an antenna 'flip' from the forward to backward state in biological and robotic experiments. (A) Sequence of a flip from a non-treated, intact (control) cockroach antenna. The antenna is initially in a forward-projecting state. As the wall moves, the antenna catches and flips to a backward-projecting state. (B) Proportion of flips between non-treated and treated cockroach antennae. The proportion of non-laser-treated (intact) antennae that flipped was statistically higher than for treated antennae ( $*P < 0.001$ ). (C,D) Data from individual joint angle sensors from the robotic antenna during an experimental trial from the initial time,  $t_0$ , until  $t_{final}$ , where  $d$  is the distance between the base of the antenna and the wall. A flip is registered when the anchored segment (most distal) is perpendicular to the wall. In C, at  $t_{flip}$  the distally oriented hairs engage with the wall, which results in the antenna transitioning (yellow) from a forward (pink)- to a backward (green)-projecting position. During this trial the wall was covered with rough felt cloth and the hairs were oriented distally. In D, the wall was covered with felt cloth and the three distal-most hairs of the robotic antenna were removed. This panel shows a failed transition from experimental data as the antenna remains forward projecting (pink) during the entire trial (arrow). (E) Data from one trial in which robotic antennal hairs ipsilateral to the wall were pointing distally while those on the other side were pointing proximally. After the antenna flipped, the proximally pointing hairs engaged, causing the contact point to move behind the base and thus significantly affecting the preview distance.

point initially moved with the same velocity as the base, remaining well ahead and thus providing an effective preview distance. From this observation, we hypothesized that distally pointing hairs are crucial in maintaining a wall contact point well ahead of the animal or robot on rough surfaces. For smoother surfaces, we would expect the coefficient of friction to become more important. To test the hypothesis that distally pointing hairs are crucial to maintain an effective preview distance, we performed an additional experiment in which the side of the antenna ipsilateral to the wall had distally pointing hairs while the other side had proximally pointing hairs. When the antenna flipped, the proximally pointing hairs came into contact with the wall, pointing toward the direction of movement. In all trials (10/10), the preview distance relative to the base became negative after the flip (Fig. 7E). These results demonstrate the importance of distally pointing hairs in maintaining an adequate preview distance following a flip on rough surfaces. Similarly, we would expect unidirectional friction to be an important property affecting preview distance on smoother surfaces.

## DISCUSSION

### Locomotion-mediated tactile sensing

How animals integrate noisy sensory information with a dynamic body during rapid locomotor tasks where neural bandwidth limitations and conduction delays impose severe constraints on control remains a challenge in neuromechanics. We discovered that during high-speed wall following, cockroaches' active antennal reconfiguration uses the energy from locomotion rather than energy generated by muscles directly associated with the sensor (Fig. 1A). Reconfiguration through running relies on the passive properties of the antenna to position the sensor in its most effective mechanical state – bent backward (Fig. 1B). A newly discovered mechanical function for antennal hairs, previously described exclusively as sensory structures (Schafer and Sanchez, 1973; Schaller, 1978), results from hairs interlocking with rough walls to produce the bent state. We abstract this reconfiguration by showing distinct mechanical states  $x_1$  (forward) and  $x_2$  (backward) that are 'switched' by an interaction among locomotion as the self-generated energy source, a mechanically tuned passive sensor and

the environment (Fig. 1B). These states can in turn affect the information  $I(x_n)$  available to the neural controller, which informs how the motor system modifies movement. We contend that during locomotor tasks where bandwidth limitations and neural conduction delays become significant, animals can shift control to the mechanics of their sensor for effective tactile sensing.

In contrast to previous studies on slow, exploratory active sensing with antennae in arthropods such as in cockroaches (Comer et al., 2003; Okada and Toh, 2004; Harley et al., 2009), crayfish (Basil and Sandeman, 2000) and stick insects (Dürr et al., 2001), here we show explicitly that body movement and sensor mechanics work synergistically in the sensing task and that the sensor is reconfigured as a result of this interaction. Previous studies during slow, exploratory active sensing tasks have shown the importance of integrating body, movement and sensor (Chiel et al., 2009), but we are not aware of any studies demonstrating the case in Fig. 1A where the energy from locomotion is transferred to the sensor, enabling it to reconfigure itself for the task of high-speed tactile navigation.

The effect of a tactile sensor's mechanical state and its interaction with the environment has also been studied in whisking in rats. It has recently been shown that a whisker can transmit different forces based on whether it hits the convex or concave side first, which could have important implications for sensory processing (Quist and Hartmann, 2012). Specifically Quist and Hartmann showed that when an applied force makes contact on the convex side on a whisker, the magnitude of the axial force generated is higher when compared with the same force applied to the concave side (Quist and Hartmann, 2012). Trigeminal ganglion neurons are known to be very sensitive to axial forces, therefore this biomechanical filtering, which depends on the force direction, could have important implications for sensing and behavior (Quist and Hartmann, 2012). Although whiskers, unlike arthropod antennae, are non-sensate along their length, rich sensory information about the spatial properties of an object can be extracted such as surface texture, object size and shape by sensing at the base of the vibrissae (Diamond et al., 2008; Vincent, 1912; Carvell and Simons, 1990). Our results are related in that we observed a change in behavior depending on whether the ipsilateral antenna was concave or convex relative to the wall, with the applied force being a normal force generated from the wall surface. While these results from mechanical properties of whiskers have not yet been linked directly to behavior and control as we have done here in the cockroach, we suspect that similar principles may apply and may be an interesting avenue for investigation.

#### Antennal mechanical state affects control strategy

Our previous control theoretic model of antenna-mediated wall following predicted that control is more challenging as the velocity increases and simpler with a greater preview distance (i.e. a longer antenna) (Cowan et al., 2006). In the present study, when wall-following cockroaches were presented with smoother and rougher walls, we found that the antenna could assume two states: projecting backward and forward (Fig. 5A). This result suggested that the transition between the observed antennal mechanical states was mediated by the mechanical properties of the environment coupled with locomotion. To understand how the environment affects antennal state, we compared the antennal posture of wall-following cockroaches running along smoother and rougher surfaces, and found significant differences in the proportions of forward- and backward-projecting antennae (Fig. 5B). Furthermore, by comparing transition probabilities for a simple two-state Markov chain, we found that transition probabilities were significantly different when the antenna occupied a forward state when comparing smoother and rougher walls (Fig. 5C).

Using predictions from a control-theoretic model of wall following, we hypothesized that a forward state would give the cockroach a greater preview distance by geometry alone; thus, we predicted that wall following control would be easier according to the model developed by Cowan and colleagues (Cowan et al., 2006). By comparing body-to-wall distance, a putative state variable for control of wall following hypothesized by Cowan and colleagues (Cowan et al., 2006), we showed that animals running at similar speeds with an antenna projecting forward ran on average closer to the wall compared with those running with an antenna projecting backward (Fig. 6A,B). This change in body-to-wall distance corresponds to approximately a whole body width of *P. americana*. Interestingly, the body-to-wall distance for cockroaches running in the bent-forward antenna state is similar to that measured for cockroaches running with an ablated antennae ipsilateral to the wall (Camhi and Johnson, 1999), thus suggesting that the mechanical state potentially affects the encoding of information and the strategy that the animals are employing. Furthermore, we determined that dynamic changes in the state of the antenna were correlated with changes in wall-following tracking behavior, specifically the initiation of body turns. Changes in mean body angle following a flip were statistically significant between the flip and control data (Fig. 6D,E).

To determine whether this change in tracking strategy could have important consequences for wall-following performance, we tracked the frequency of leg and body contact for both cases. Our results showed a significant difference in the proportion of leg and body contact associated with the antenna state (Fig. 6C). We observed that both leg and body contact, but especially body contact, were linked with body-to-wall collisions, often leading to a decrease in speed due to body redirection. We found the median change in velocity to be  $-7.48 \text{ cm s}^{-1}$  when comparing approximately two strides before and after contact. Our observations and measurement on wall collisions are in agreement with observations described previously (Baba et al., 2010). Baba and colleagues noted that cockroaches that ran sufficiently close to the wall 'touched it with their body and this sometimes cause[d] them to fall' (Baba et al., 2010). In summary, for animals running with their antenna projecting forward, we observed marked changes in behavioral strategy including increased leg and body contact and wall collision leading to significant decreases in speed. Our results raise the possibility that increased leg contact could allow a cockroach to sense the wall with its legs, thus relying on different sensory modalities (e.g. tarsus or leg hair contact) for thigmotaxis, as suggested previously (Camhi and Johnson, 1999). Employing a strategy that relies on leg and body contact for sensing comes with a cost: the increased probability of body decelerations due to collisions with clear consequences when placed within the context of high-speed predator evasion. In conclusion, our results do not support the hypothesis that an increased preview distance afforded by a forward-projecting antenna leads to improved wall following. In fact, tracking performance and task-level control were superior with a backward-projecting antenna. However, it remains unclear whether body-to-wall distance information can be sensed by the antenna when it is in a forward-projecting state. After demonstrating that the antenna state is crucial for task-level control, we hypothesized that the mechanical tuning of the antenna – and in particular the mechanical role played by sensory hairs – may enable passive switching to the backward-projecting state.

#### Mechanical role of sensory hairs

We showed that passive antenna hairs coupled with forward motion are sufficient to allow an antenna to transition to a different

mechanical state by selectively ablating mechanosensory hairs using a high-precision laser system (Fig. 3). By displacing a fixed animal with its antenna projecting forward against a wall surface, we showed that we could reproduce the forward- to backward-projecting sensor reconfiguration observed in the running animal. A repeat of the experiment with ablated hairs demonstrated that hairs play an important role in the reconfiguration (Fig. 7B). Effectively, we showed that a distributed hair array on a sensor is effective at allowing the sensory appendage to 'stick' to a substrate by interlocking. Small, distributed hairs are especially effective as the ability of hairs to engage in asperities increases as the radius of the tip decreases (Asbeck et al., 2006).

The role of directionally tuned hair arrays has previously been studied during high-speed terrestrial locomotion in cockroaches, spiders and crabs (Spagna et al., 2007). Leg hairs or spines were shown to function as distributed contact points by increasing the probability of foot engagement when animals ran over terrain with sparse contacts. Cockroaches, spiders and crabs running at high speed attained increased mobility with collapsible spines without any detectable changes in neural feedback. Spagna and colleagues provided evidence for a novel mechanical function for these spines, which were thought to only play a role in sensing (Spagna et al., 2007). Similarly, in the present study we discovered that hairs on antennae, also once thought to only play a role in sensing, have a new function that is mechanical. Specifically, hairs can mechanically interlock with surfaces and allow the antenna to adopt a different configuration when coupled with locomotion. The study on leg spines reinforced the importance of integrating passive mechanics to understand the principles of stability and maneuverability in high-speed terrestrial locomotion when the neuromechanical system is pushed near its limits (Full and Koditschek, 1999). Analogously, we provide support that understanding the biomechanical processing of sensory appendages prior to neural transduction is crucial to understanding sensorimotor integration during rapid behaviors (Sane and McHenry, 2009). While we found that the properties of the surface can influence the mechanical state of the antenna, it is important to note that another variable involved is the angle of attack of the antenna flagellum with respect to the wall as noted by Camhi and Johnson (Camhi and Johnson, 1999). However, we found that the angle of attack of the flagellum did not affect the likelihood of antenna reconfiguration or flipping in intact antennae, thus supporting the hypothesis that antennal biomechanics are the predominant factor influencing antennal configuration (Fig. 1). These results were corroborated by the robotic experiment testing the sensitivity of base angle. While antennal reconfiguration at the tip is robust to changes in base angle, it remains an open question to what extent cockroaches precisely control antennal muscles during the task of high-speed wall following. In future studies it will be important to carefully examine the effect of antennal abduction angle on turning, as studies during slow, exploratory behavior have shown that proprioceptors at the base affect tactile orientation (Okada and Toh, 2000).

Finally, our biological results lead to a directly testable neurobiological hypothesis. Specifically, we hypothesize that the mechanical state of the antenna may affect sensory processing and subsequently affect the information available to the neural controller downstream. Recording directly from the antenna nerve in a virtual turning experiment as developed by Lee and colleagues (Lee et al., 2008) within the control theoretic context developed by Cowan and colleagues (Cowan et al., 2006) could reveal how sensory processing is influenced by the interaction between the antenna and a wall projection.

#### Physical model of antenna provides insight on preview distance

To further explore biomechanical factors that may influence the process of antenna reconfiguration, we built a tunable physical model of an arthropod antenna inspired by the American cockroach (Fig. 4) (Demir et al., 2010). This physical model allowed us to manipulate mechanical parameters that would otherwise be difficult or impossible to test in animals. In our experimental trials, we considered different initial conditions for wall roughness, hair geometry and orientation for a constant antenna length, antenna stiffness, base angle, base velocity and wall distance. We showed that the robotic antenna's flipping statistics were categorically affected by the existence of appropriately oriented hairs for a given wall roughness (Fig. 7C,D). Distally projecting hairs tended to anchor themselves immediately, and the shear forces at the surface easily overcame the inter-segmental joint stiffness along the antenna. As the base moved at constant velocity, the joint angles changed continually either until the distal segments became perpendicular to the wall (flip) or until the shear forces between the distal segments and the wall overcame the hair-asperity contact strength (no flip). These results from the physical model confirm that distally pointing hairs increase the probability of engaging wall asperities, which constitutes the main physical interaction in mediating the flip on rough surfaces.

In addition, the physical model provided new biological insight. We showed that for rough surfaces, distally pointing hairs, following reconfiguration, are crucial in maintaining an adequate preview distance such that the contact point can remain well ahead of the linear actuator base or 'head' (Fig. 7E). We suspect that for rougher surfaces, hair-asperity engagement will dominate whereas for smoother surfaces the coefficient of friction will become more important. Thus, for smoother surfaces unidirectional friction will be an important factor influencing preview distance. Preview distance is a crucial parameter for stable high-speed tactile navigation, as rigorously demonstrated in a neuromechanical model of wall following using realistic cockroach running dynamics (Lee et al., 2008). We propose that distally pointing hairs for rough surfaces and unidirectional friction for smooth surfaces along with properly tuned mechanics (i.e. flexural stiffness profile) are important mechanical parameters that influence preview distance.

In future studies, it will be essential to further explore the design space for building an effective tactile sensor on a dynamic, mobile robot. For example, the backward-projecting 'inverted-J' antenna shape may be more effective for following surfaces with asperities and/or obstacles. We hypothesize that this shape may significantly decrease the probability of the antenna becoming wedged into surface asperities, which may have important implications for sensing. Some of the advantages of this geometry have been successfully tested in a bio-inspired wall-following robot (Lee et al., 2008). We speculate that the bent-backward geometry can increase the effective preview sensory volume (Snyder et al., 2007) available to a surface-following robot by increasing the probability of contact ahead. However, there is an important design trade-off in the backward-projecting geometry that will need to be explored further. Specifically, the potential advantages of this shape come at the cost of decreasing preview distance. Finally, it will be necessary to investigate the effect of the antennal stiffness profile during wall following and/or surface contour extraction tasks. Preliminary results from Demir and colleagues suggest that a more compliant tip – i.e. a decreasing stiffness profile – can help resolve finer details (higher spatial frequencies) during a contour extraction task (Demir et al., 2010). Studies on the biomechanics of arthropod antennae such as in crayfish (Sandeman, 1989) and stick insects (Dirks and Dürr, 2011) are consistent with a



decreasing flexural stiffness from base to tip. While from geometry we expect similar mechanical properties in *P. americana* (Kapitskii, 1984), further mechanical testing will be necessary.

From an engineering point of view, we have shown that distally oriented hairs can facilitate a change of mechanical state of a physical model of an antenna when coupled with forward motion. In addition, on rough surfaces, distally pointing hairs allow the antenna to maintain an effective preview distance following reconfiguration. This is an important advance in bio-inspired antenna design for mobile robotic applications as it provides a mechanism that relies on passive mechanics and locomotion without relying on actuated sensor control. Further studies will need to determine the effect of tactile sensor configuration on high-speed wall-following performance and the feasibility of the flipping mechanism on mobile robots. This mechanism may afford a robust solution for mobile robots operating in challenging environments for search and rescue operations, and exploration where sonar- and vision-based sensors may be insufficient.

### ACKNOWLEDGEMENTS

We thank Anil Mahavadi, Brian McRae, Vladislav Bely and Avantika Pathak for laboratory assistance. We thank Kaushik Jayaram and Simon Sponberg for helpful discussions. We thank Paul Birkmeyer, Andrew Gillies and Ron Fearing of the Biomimetic Millisystems Lab at UC Berkeley for help with the laser ablation experiments. We thank Linh Tran for help with statistical analysis.

### AUTHOR CONTRIBUTIONS

J.-M.M., A.D., J.L., N.J.C. and R.J.F. designed the experiments. J.-M.M., A.D. and J.L. conducted experiments and analysed the data. J.-M.M., A.D., N.J.C. and R.J.F. wrote the manuscript.

### COMPETING INTERESTS

No competing interests declared.

### FUNDING

This material is based upon work supported by the National Science Foundation (NSF) [Graduate Research Fellowship to J.-M.M.; Integrative Graduate Education and Research Traineeship Program 0903711 to R.J.F. and J.-M.M., CISE-0845749 to N.J.C. and A.D.]; and the United States Army Research Laboratory [Micro Autonomous Systems and Technology Collaborative Technology Alliance W911NF-08-2-0004 to R.J.F.].

### REFERENCES

- Asbeck, A. T., Kim, S., Cutkosky, M. R., Provancher, W. R. and Lanzetta, M. (2006). Scaling hard vertical surfaces with compliant microspine arrays. *Int. J. Robot. Res.* **25**, 1165-1179.
- Baba, Y., Tsukada, A. and Comer, C. M. (2010). Collision avoidance by running insects: antennal guidance in cockroaches. *J. Exp. Biol.* **213**, 2294-2302.
- Bajcsy, R. (1988). Active Perception. *Proc. IEEE* **76**, 966-1005.
- Basil, J. and Sandeman, D. (2000). Crayfish (*Cherax destructor*) use tactile cues to detect and learn topographical changes in their environment. *Ethology* **106**, 247-259.
- Bell, W., Roth, W. J. and Louis, M. (2007). *Cockroaches: Ecology, Behavior and Natural History*, pp. 39. Johns Hopkins University, MD: Johns Hopkins University Press.
- Camhi, J. M. and Johnson, E. N. (1999). High-frequency steering maneuvers mediated by tactile cues: antennal wall-following in the cockroach. *J. Exp. Biol.* **202**, 631-643.
- Carvell, G. E. and Simons, D. J. (1990). Biometric analyses of vibrissal tactile discrimination in the rat. *J. Neurosci.* **10**, 2638-2648.
- Chiel, H. J., Ting, L. H., Ekeberg, O. and Hartmann, M. J. Z. (2009). The brain in its body: motor control and sensing in a biomechanical context. *J. Neurosci.* **29**, 12807-12814.
- Coles, R. B. and Guppy, A. (1988). Directional hearing in the barn owl (*Tyto alba*). *J. Comp. Physiol. A* **163**, 117-133.
- Comer, C. M., Parks, L., Halvorsen, M. B. and Breese-Terteling, A. (2003). The antennal system and cockroach evasive behavior. II. Stimulus identification and localization are separable antennal functions. *J. Comp. Physiol. A* **189**, 97-103.
- Cowan, N. J., Lee, J. and Full, R. J. (2006). Task-level control of rapid wall following in the American cockroach. *J. Exp. Biol.* **209**, 1617-1629.
- Demir, A., Samson, E. and Cowan, N. J. (2010). A tunable physical model of arthropod antennae. *IEEE Int. Conf. Robot. Autom.* 3793-3798.
- Diamond, M. E., von Heimendahl, M., Knutsen, P. M., Kleinfeld, D. and Ahissar, E. (2008). 'Where' and 'what' in the whisker sensorimotor system. *Nat. Rev. Neurosci.* **9**, 601-612.
- Dickinson, M. H. (2005). The initiation and control of rapid flight maneuvers in fruit flies. *Integr. Comp. Biol.* **45**, 274-281.
- Dirks, J. H. and Dür, V. (2011). Biomechanics of the stick insect antenna: damping properties and structural correlates of the cuticle. *J. Mech. Behav. Biomed. Mater.* **4**, 2031-2042.
- Dür, V., König, Y. and Kittmann, R. (2001). The antennal motor system of the stick insect *Carausius morosus*: anatomy and antennal movement pattern during walking. *J. Comp. Physiol. A* **187**, 131-144.
- Egelhaaf, M., Kern, R., Krapp, H. G., Kretzberg, J., Kurtz, R. and Warzecha, A. K. (2002). Neural encoding of behaviourally relevant visual-motion information in the fly. *Trends Neurosci.* **25**, 96-102.
- Elzinga, M. J., Dickson, W. B. and Dickinson, M. H. (2012). The influence of sensory delay on the yaw dynamics of a flapping insect. *J. R. Soc. Interface* **9**, 1685-1696.
- Full, R. J. and Koditschek, D. (1999). Template and anchors: neuromechanical hypotheses of legged locomotion on land. *J. Exp. Biol.* **202**, 3325-3332.
- Harley, C. M., English, B. A. and Ritzmann, R. E. (2009). Characterization of obstacle negotiation behaviors in the cockroach, *Blaberus discoidalis*. *J. Exp. Biol.* **212**, 1463-1476.
- Hartmann, M. (2001). Active sensing capabilities of the rat whisker system. *Auton. Robots* **11**, 249-254.
- Holmes, P., Full, R. J., Koditschek, D. E. and Guckenheimer, J. (2006). The dynamics of legged locomotion: models, analyses, and challenges. *SIAM Rev. Soc. Ind. Appl. Math.* **48**, 207-304.
- Kapitskii, S. V. (1984). Morphology of the antenna of the male American cockroach *Periplaneta americana*. *J. Evol. Biochem. Physiol.* **20**, 59-66.
- Koehl, M. A., Koseff, J. R., Crimaldi, J. P., McCay, M. G., Cooper, T., Wiley, M. B. and Moore, P. A. (2001). Lobster sniffing: antennule design and hydrodynamic filtering of information in an odor plume. *Science* **294**, 1948-1951.
- Lee, J., Sponberg, S. N., Loh, O. Y., Lamperski, A. G., Full, R. J. and Cowan, N. J. (2008). Templates and anchors for antenna-based wall following in cockroaches and robots. *IEEE Trans. Robot.* **24**, 130-143.
- More, H. L., Hutchinson, J. R., Collins, D. F., Weber, D. J., Aung, S. K. H. and Donelan, J. M. (2010). Scaling of sensorimotor control in terrestrial mammals. *Proc. R. Soc. B* **277**, 3563-3568.
- Nelson, M. E. and MacIver, M. A. (2006). Sensory acquisition in active sensing systems. *J. Comp. Physiol. A* **192**, 573-586.
- Okada, J. and Toh, Y. (2000). The role of antennal hair plates in object-guided tactile orientation of the cockroach (*Periplaneta americana*). *J. Comp. Physiol. A* **186**, 849-857.
- Okada, J. and Toh, Y. (2004). Antennal system in cockroaches: a biological model of active tactile sensing. *Int. Congr. Ser.* **1269**, 57-60.
- Olberg, R. M., Worthington, A. H. and Venator, K. R. (2000). Prey pursuit and interception in dragonflies. *J. Comp. Physiol. A* **186**, 155-162.
- Polak, M. and Rashed, A. (2010). Microscale laser surgery reveals adaptive function of male intromittent genitalia. *Proc. R. Soc. B* **277**, 1371-1376.
- Prescott, T. J., Diamond, M. E. and Wing, A. M. (2011). Active touch sensing. *Philos. Trans. R. Soc. B* **366**, 2989-2995.
- Quist, B. W. and Hartmann, M. J. Z. (2012). Mechanical signals at the base of a rat vibrissa: the effect of intrinsic vibrissa curvature and implications for tactile exploration. *J. Neurophysiol.* **107**, 2298-2312.
- Sandeman, D. (1989). Physical properties, sensory receptors and the tactile reflexes of the antenna of the Australian freshwater crayfish *Cherax destructor*. *J. Exp. Biol.* **141**, 197-217.
- Sane, S. P. and McHenry, M. J. (2009). The biomechanics of sensory organs. *Integr. Comp. Biol.* **49**, i8-i23.
- Schafer, R. and Sanchez, T. V. (1973). Antennal sensory system of the cockroach, *Periplaneta americana*: postembryonic development and morphology of the sense organs. *J. Comp. Neurol.* **149**, 335-353.
- Schaller, D. (1978). Antennal sensory system of *Periplaneta americana* L.: distribution and frequency of morphologic types of sensilla and their sex-specific changes during postembryonic development. *Cell Tissue Res.* **191**, 121-139.
- Seelinger, G. (1984). Sex-specific activity patterns in *Periplaneta americana* and their relation to mate-finding. *Z. Tierpsychol.* **65**, 309-326.
- Snyder, J. B., Nelson, M. E., Burdick, J. W. and Maciver, M. A. (2007). Omnidirectional sensory and motor volumes in electric fish. *PLoS Biol.* **5**, e301.
- Spagna, J. C., Goldman, D. I., Lin, P.-C., Koditschek, D. E. and Full, R. J. (2007). Distributed mechanical feedback in arthropods and robots simplifies control of rapid running on challenging terrain. *Bioinspir. Biomim.* **2**, 9-18.
- Staudacher, E., Gebhardt, M. and Durr, V. (2005). Antennal movements and mechanoreception: neurobiology of active tactile sensors. *Adv. Insect Physiol.* **32**, 49-205.
- Vincent, S. B. (1912). The function of the vibrissae in the behavior of the white rat. *Behav. Monographs* **1**, 1-82.
- Wotton, J. M., Haresign, T. and Simmons, J. A. (1995). Spatially dependent acoustic cues generated by the external ear of the big brown bat, *Eptesicus fuscus*. *J. Acoust. Soc. Am.* **98**, 1423-1445.